

# Theoretical Prediction and Experimental Tests of Conformational Switches in Transition States of Diels–Alder and 1,3-Dipolar Cycloadditions to Enol Ethers

Jian Liu, Satomi Niwayama, Ying You, and K. N. Houk\*

Department of Chemistry and Biochemistry, University of California, Los Angeles, California 90095

Received July 30, 1997

Transition structures for the cycloadditions of butadiene, acrolein, nitrosoethylene, and methyl-enenitrone to 1-butene, silyl vinyl ether, and methyl vinyl ether have been located using ab initio RHF theory with the 3-21G basis set and with density functional theory using the Becke3LYP functional and the 6-31G\* basis set. The computational results show that there is a switch in the conformation of the enol ether from syn (COCC = 0°), which is favored by 2.3 kcal/mol in the reactant, to anti (COCC = 180°), which is favored by 1.2–6.6 kcal/mol in the various transition structures studied here. The results are consistent with the experimental stereoselectivities in reactions of chiral enol ethers observed by Denmark and Reissig. The preference of the anti conformation in the transition structures is due primarily to electrostatic effects and, to a lesser extent, steric effects. The preference is predicted to be influenced significantly by polar solvents. The magnitude of this preference was calculated theoretically and measured experimentally: the rates of cycloadditions of conformationally fixed enol ethers, 2,3-dihydrofuran and 2-methylene-tetrahydrofuran, with 1-nitroso-1-phenylethylene and with *C*-benzoyl-*N*-phenylnitrone were studied. Observed relative rates are in good agreement with prediction and confirm that enol ethers adopt the *s*-trans conformation in transition states of cycloadditions.

## Introduction

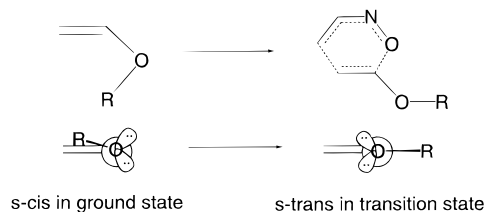
Enol ethers have been used in inverse electron-demand Diels–Alder and 1,3-dipolar cycloadditions for the synthesis of five- and six-membered ring systems in natural products.<sup>1</sup> Previous theoretical studies on the stereoselectivity focused mainly on the endo/exo selectivity of these cycloaddition reactions.<sup>2</sup> The goal of our investigation was to determine the effect of dienophile conformations on the rates and stereoselectivities of these types of cycloadditions. We have discovered a general phenomenon for the cycloaddition reactions of enol ethers, in which a clear-cut “conformational switch” occurs

(1) Diels–Alder reactions: (a) Denmark, S. E.; Thorarensen, A. *Chem. Rev. (Washington, D.C.)* **1996**, *96*, 137 and references therein. (b) Boger, D. L. *Chemtracts* **1996**, *9*, 149 and references therein. (c) Denmark, S. E.; Dappen, M. S.; Sternberg, J. A. *J. Org. Chem.* **1984**, *49*, 4741. (d) Tietze, L.-F.; Gluesenkamp, K.-H.; Harms, K.; Remberg, G. *Tetrahedron Lett.* **1982**, *23*, 1147. (e) Arnold, T.; Orschel, B.; Reissig, H.-U. *Angew. Chem., Int. Ed. Engl.* **1992**, *31*, 1033. (f) Hippeli, C.; Reissig, H.-U. *Liebigs Ann. Chem.* **1990**, 217. (g) Zimmer, R.; Reissig, H.-U. *Liebigs Ann. Chem.* **1991**, 553. (h) Zimmer, R.; Reissig, H.-U. *J. Org. Chem.* **1992**, *57*, 339. (i) Fisera, T.; Dandarava, M.; Kovac, J.; Gaplovsky, A.; et al. *Collect. Czech. Chem. Commun.* **1982**, *47*, 523. 1,3-Dipolar cycloadditions: (j) *Nitrones, Nitronates and Nitroxides*; Wiley: New York, 1990; pp 1–104. (k) Annunziata, R.; Cinquini, M.; Cozzi, F.; Raimondi, L. *Gazz. Chim. Ital.* **1989**, *119*, 253.

(2) (a) Desimoni, G.; Colombo, G.; Righetti, P. P.; Tacconi, G. *Tetrahedron* **1973**, *29*, 2635. (b) Reissig, H.-U.; Hippeli, C.; Arnold, T. *Chem. Ber.* **1990**, *123*, 2403. (c) McCarrick, M. A.; Wu, Y.-D.; Houk, K. N. *J. Org. Chem.* **1993**, *58*, 3330. (d) Gouverneur, V. E.; Houk, K. N.; Pascual-Teresa, B.; Beno, B.; Janda, K. D.; Lerner, R. A. *Science* **1993**, *262*, 204. (e) Rastelli, Q.; Bagatti, M.; Gandolfi, R.; Burdisso, M. *J. Chem. Soc., Faraday Trans.* **1994**, *90*, 1077. (f) Sisti, N. J.; Motorina, I. A.; Dau, M. T. H.; Riche, C.; Fowler, F. W.; Grierson, D. S. *J. Org. Chem.* **1996**, *61*, 3715. (g) Dharale, D. D.; Trombini, C. *J. Chem. Soc., Chem. Commun.* **1992**, 1268.

(3) Other conformational switches can be found in nucleophilic additions to carbonyl compounds (Coxon, J. M.; Houk, K. N.; Luihrand, R. T. *J. Org. Chem.* **1995**, *60*, 418 and references therein) and in nitrile oxide cycloadditions to chiral alkenes (Houk, K. N.; Duh, H.-Y.; Wu, Y.-D.; Moses, S. R. *J. Am. Chem. Soc.* **1986**, *108*, 2754).

## Scheme 1



during the course of reaction.<sup>3</sup> Thus, the ground-state conformation of the reactant is changed to a dramatically different conformation in the transition structure (Scheme 1). This conformational switch reverses the sense of  $\pi$ -facial stereoselectivity of reactions of chiral enol ethers from that which would be expected on the basis of facial accessibility in the ground state. The results provide an explanation for the stereoselectivities of cycloadditions of chiral enol ethers reported by Denmark et al., Reissig et al., and others.<sup>4</sup>

The stereoselectivities of addition reactions are sometimes rationalized in terms of steric or torsional effects involving the reactant conformation.<sup>5</sup> This explanation is satisfactory for reactions when the conformation of the transition structures mimics that of the reactants; however, the Curtin–Hammett principle shows that this will not always be the case.<sup>6</sup> There are many examples where consideration of the ground state leads to successful rationalization of the reaction stereoselectivity, but there

(4) (a) Arnold, T.; Reissig, H.-U. *Synlett* **1990**, 514. (b) Denmark, S. E.; Thorarensen, A. *J. Org. Chem.* **1994**, *59*, 5672. (c) Denmark, S. E.; Schnute, M. E.; Marcin, L. R.; Thorarensen, A. *J. Org. Chem.* **1995**, *60*, 3205. (d) Denmark, S. E.; Thorarensen, A.; Middle, D. S. *J. Org. Chem.* **1995**, *60*, 3574.

(5) (a) Toromanoff, E. *Tetrahedron* **1981**, *37*, 3141. (b) Bucourt, R. *Top. Stereochem.* **1974**, *8*, 159.

(6) Seeman, J. I. *Chem. Rev. (Washington, D.C.)* **1983**, *83*, 84.

are others where there is a switch in conformation in the transition structures as compared to that of the reactants.<sup>7</sup> We have predicted theoretically, and have verified experimentally through studies of rates of cycloadditions of some conformationally fixed enol ethers, that such a conformational switch occurs.

### Calculation Methods

Geometry optimizations were carried out at the restricted Hartree–Fock (RHF) level and with density functional theory (DFT) and the Becke3LYP<sup>8</sup> functional using the GAUSSIAN94 program.<sup>9</sup> For the reactions with ethylene, 1-butene, silyl vinyl ether, and methyl vinyl ether, the reactants and transition structures were fully optimized with the 3-21G basis set for RHF and with the 6-31G\* basis set for Becke3LYP calculations. For the reactions with conformationally fixed dienophiles and dipolarophiles, the reactants and transition structures were fully optimized at the RHF level with the 3-21G basis set. Each of the transition structures gave only one imaginary harmonic vibrational frequency, corresponding to the formation of the C–C and C–X bonds. The self-consistent reaction field (SCRFF)<sup>10</sup> cavity model with the SCIPCM option<sup>11</sup> was used to calculate the solvation energies of the gas-phase-optimized structures in order to establish the effect of solvent on the reaction rates and stereoselectivities. The reported charges are Mulliken charges.

### Results and Discussion

**1. Theoretical Prediction of the Conformational Switch in Cycloadditions of Enol Ethers. Conformations of Vinyl Ethers and 1-Butene in Ground States.** The lowest energy conformation of methyl vinyl ether is the *s-cis* planar conformation, as demonstrated by both experiment and theory.<sup>12</sup> The *s-trans* conformation is nearly 2.0 kcal/mol higher in energy. This preference is further supported by RHF/3-21G and Becke3LYP/6-31G\* calculations. Table 1 lists the calculated and relative energies of *s-cis* and *s-trans* methyl vinyl ether, silyl vinyl ether, and 1-butene. Although the bulky silyl group decreases the preference for the *s-cis* conformation because of steric hindrance, the *s-trans* conformation is still 1.5 kcal/mol higher in energy by RHF and 0.7 kcal/mol by DFT. The *s-cis* preference can be explained in terms of electrostatic effects: the lone pair electrons on the oxygen avoid the  $\pi$  electrons of the

**Table 1. Calculated Energies (au) and Relative Energies (kcal/mol, in Parentheses) of *s-Cis* and *s-Trans* Alkenes by RHF/3-21G and Becke3LYP/6-31G\* Methods**

olefins	RHF/3-21G	Becke3LYP/6-31G*
<i>s-cis</i> methyl vinyl ether	–190.855 30 (0.0)	–193.114 06 (0.0)
<i>s-trans</i> methyl vinyl ether	–190.850 10 (3.3)	–193.110 42 (2.3)
<i>s-cis</i> silyl vinyl ether	–440.634 47 (0.0)	–444.534 41 (0.0)
<i>s-trans</i> silyl vinyl ether	–440.631 09 (1.5)	–444.533 25 (0.7)
<i>s-cis</i> 1-butene	–155.241 94 (0.8)	–157.220 38 (0.4)
<i>s-trans</i> 1-butene	–155.243 26 (0.0)	–157.221 07 (0.0)

double bond in the *s-cis* conformation.<sup>12</sup> Consequently, the dipole moment of the molecule is small. In 1-butene, the *s-cis* conformation is a local minimum but lies 0.8 kcal/mol above the *gauche* minimum; here there are no significant electrostatic effects and steric hindrance destabilizes the *s-cis* conformer relative to the *s-trans* conformer.

**Transition Structures for the Cycloaddition Reactions of Nitrosoethylene, Acrolein, Butadiene, and Nitron with Ethylene.** Calculations for each of these systems have been reported using a variety of different methods.<sup>13</sup> The cycloadditions involving nitron and acrolein reacting with ethylene have been studied using low-level *ab initio* methods or semiempirical methods, while those with butadiene<sup>13c</sup> and nitrosoethylene<sup>13j,k</sup> have been studied using higher levels of theory such as Becke3LYP/6-31G\* and MP2/6-31G\*.

Concerted asynchronous transition structures were found for both Diels–Alder and 1,3-dipolar cycloadditions by RHF and DFT methods in our calculations. Previous studies on related cycloadditions have predicted concerted transition structures with geometries similar to those found here.<sup>13</sup> The transition structures for the reactions of nitrosoethylene, acrolein, butadiene, and nitron with ethylene have been located using RHF/3-21G and Becke3LYP/6-31G\* methods in order to allow comparison with the cycloadditions of substituted dienophiles or dipolarophiles. Figure 1 shows the geometries of the four transition structures and the activation energies predicted by these two methods. The activation energy predicted for the cycloaddition of butadiene with ethylene is 24.8 kcal/mol (Becke3LYP/6-31G\* with ZPE included),<sup>13c</sup> which agrees remarkably well with the experimental value of  $27.5 \pm 2$  kcal/mol.<sup>14</sup> The acrolein activation energy is roughly the same. Nitrosoethylene is predicted to be a much more reactive diene than acrolein in the inverse electron-demand Diels–Alder reactions, also in agreement with experiment.<sup>15</sup> The reactivities are normally controlled by LUMO<sub>diene</sub>–HOMO<sub>dienophile</sub> interactions for these two inverse electron-demand Diels–Alder reactions. There is 0.14 electron transferred from ethylene to both acrolein and nitrosoethylene in the respective Diels–Alder reactions. Nitron should undergo 1,3-

(7) For example: Martinelli, M. J.; Peterson, B. C.; Khan, V. V.; Hutchison, D. R.; Houk, K. N. *J. Org. Chem.* **1994**, *59*, 2204.

(8) (a) Hohenberg, P.; Kohn, W. *Phys. Rev.* **1964**, *136*, B864. (b) Kohn, W.; Sham, L. J. *Phys. Rev.* **1965**, *140*, A1133. (c) Lee, C.; Yang, W.; Parr, R. G. *Phys. Rev.* **1988**, *B37*, 785. (d) Becke, A. D. *Phys. Rev.* **1988**, *A38*, 3098. (e) Michlich, B.; Savin, A.; Stoll, H.; Preuss, H. *Chem. Phys. Lett.* **1989**, *157*, 200.

(9) Gaussian94 (Revision A.1), Frisch, M. J.; Trucks, G. W.; Schlegel, H. B.; Gill, P. M. W.; Johnson, B. G.; Robb, M. A.; Cheeseman, J. A.; Keith, T. A.; Peterson, G. A.; Montgomery, J. A.; Raghavachari, K.; Al-Laham, A. A.; Zakrzewski, V. G.; Oriz, J. V.; Foresman, J. B.; Cioslowski, J.; Stefanov, B. B.; Nanayakkara, A.; Challacombe, M.; Peng, C. Y.; Ayala, P. Y.; Chen, W.; Wong, M. W.; Andres, J. L.; Replogle, E. S.; Gomperts, R.; Martin, R. L.; Fox, D. J.; Binkley, J. S.; Defrees, D. J.; Baker, J.; Stewart, J. P.; Head-Gordon, M.; Gonzalez, C.; Pople, J. A.; Gaussian Inc., Pittsburgh, PA, 1995.

(10) (a) Wong, M. W.; Frisch, M. J.; Wiberg, K. B. *J. Am. Chem. Soc.* **1991**, *113*, 4776. (b) Wong, M. W.; Wiberg, K. B.; Frisch, M. J. *J. Am. Chem. Soc.* **1992**, *114*, 523. (c) Wong, M. W.; Wiberg, K. B.; Frisch, M. J. *J. Chem. Phys.* **1991**, *95*, 8991. (d) Wong, M. W.; Wiberg, K. B.; Frisch, M. J. *J. Am. Chem. Soc.* **1992**, *114*, 1645.

(11) Wiberg, K. B.; Keith, T. A.; Frisch, M. J.; Murcko, M. *J. Phys. Chem.* **1995**, *99*, 9072.

(12) For example: (a) Owen, N. L.; Seip, H. M. *Chem. Phys. Lett.* **1968**, *48*, 162. (b) Owen, N. L.; Sheppard, N. *Trans. Faraday Soc.* **1964**, *60*, 634. (c) Cahill, P.; Gold, L. P.; Owen, N. L. *J. Chem. Phys.* **1968**, *48*, 1620. (d) Gallinella, E.; Cadioli, B. *J. Mol. Struct.* **1991**, *249*, 343.

(13) (a) Li, Y.; Houk, K. N. *J. Am. Chem. Soc.* **1993**, *115*, 7478. (b) Houk, K. N.; Gonzalez, J.; Li, Y. *Acc. Chem. Res.* **1995**, *28*, 81. (c) Goldstein, E.; Beno, B.; Houk, K. N. *J. Am. Chem. Soc.* **1996**, *118*, 6036. (d) Brown, F. K.; Singh, U. C.; Kollman, P. A.; Raimondi, L.; Houk, K. N.; Bock, C. W. *J. Org. Chem.* **1992**, *57*, 4868. (e) Houk, K. N.; Sims, J.; Watts, C.; Luskus, I. J. *J. Am. Chem. Soc.* **1973**, *95*, 7301. (f) Houk, K. N.; Sims, J.; Duke, R. E., Jr.; Strozier, R. W.; George, J. K. *J. Am. Chem. Soc.* **1973**, *95*, 7287. (g) Pascal, Y. L.; Chanet-Ray, J.; Vessiers, R.; Zeroual, A. *Tetrahedron* **1992**, *48*, 7197. (h) Lee, I.; Han, E. S.; Choi, J. Y. *J. Comput. Chem.* **1984**, *5*, 606. (i) Tietze, L. F.; Femen, J.; Anders, E. *Angew. Chem., Int. Ed. Engl.* **1989**, *28*, 1371. (j) Jursic, B. S.; Zdravkovski, Z. *J. Org. Chem.* **1995**, *60*, 3163. (k) Sperling, D.; Mehlhorn, A.; Reissig, H.-U.; Fabian, J. *Liebigs Ann.* **1996**, 1615.

(14) Rowley, D.; Steiner, H. *Discuss. Faraday Soc.* **1951**, *10*, 198.

(15) Boger, D. L. *Chem. Rev. (Washington, D.C.)* **1988**, *86*, 781 and references therein.

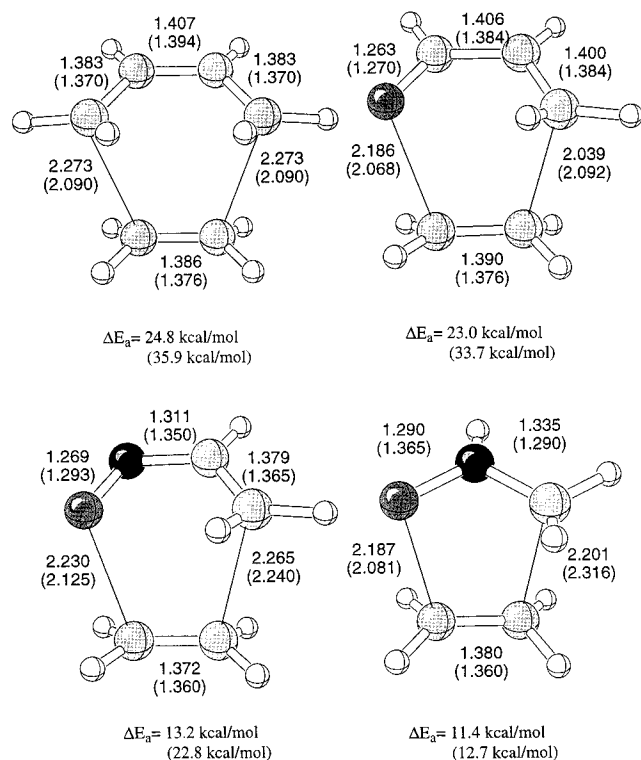
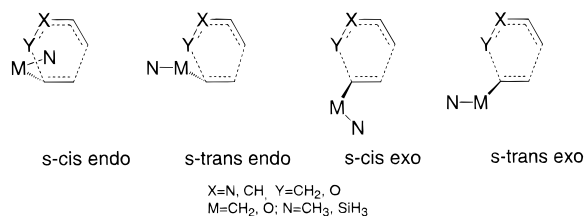


**Figure 1.** Transition structures and activation energies for the cycloadditions of ethylene with butadiene, acrolein, nitrosoethylene, and nitrone with Becke3LYP/6-31G\* and RHF/3-21G (in parentheses).

### Scheme 2



dipolar cycloadditions with alkenes very easily, as predicted by the very low activation energy of 11.4 kcal/mol, obtained at the Becke3LYP/6-31G\* level for the parent system. The charge transfer from ethylene to nitrone is only 0.02 electron in the transition state. The C–O bond lengths in the nitrosoethylene and nitrone transition structures are about only 0.02 Å shorter than the C–C bonds, while the forming C–C bond in the acrolein reaction is shorter than the forming C–O bond. However, since a normal C–O bond length (1.48 Å) is shorter than a single C–C bond length (1.54 Å), there is, nevertheless, more C–C than C–O bond formation in all of these cycloaddition transition structures.

**Transition Structures for the Cycloadditions of Methyl Vinyl Ether.** For each of the cycloadditions of methyl vinyl ether with butadiene, acrolein, nitrosoethylene, and nitrone, four transition structures could be located, referred to here as the s-cis endo, s-trans endo, s-cis exo, and s-trans exo (Scheme 2). There are only small differences in the geometries of the transition structures obtained by RHF/3-21G and B3LYP/6-31G\* methods. The relative energies of the transition structures obtained by both methods are similar, with RHF/3-21G predicting a slightly larger preference for the s-trans conformation in the transition structures. The

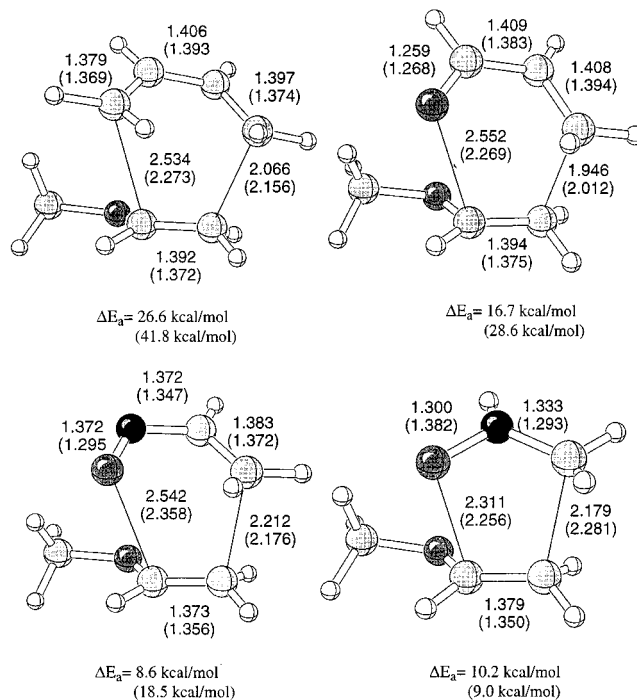


**Figure 2.** Transition structures and activation energies for the cycloaddition of methyl vinyl ether with butadiene, acrolein, nitrosoethylene, and nitrone with Becke3LYP/6-31G\* and RHF/3-21G (in parentheses).

s-trans endo transition structures with methyl vinyl ether are shown in Figure 2. The forming bond lengths in s-trans endo transition structures are similar to those found in the s-cis endo, s-trans-exo, and s-cis exo transition structures. For the inverse electron-demand Diels–Alder cycloadditions with nitrosoethylene and acrolein, the controlling frontier orbital interactions involve the LUMO(diene) and HOMO(dienophile). This is reflected in the charge transfer (B3LYP/6-31G\*) from methyl vinyl ether of 0.23 and 0.20 to nitrosoethylene and acrolein, respectively. For the cycloadditions with nitrone and butadiene, there is less charge transfer: 0.07 and 0.08 electron, respectively.

The methoxy group increases the asynchronicity measured as the difference between the bond lengths of the two forming bonds in the transition structures. The forming bonds  $\alpha$  to the methoxy group are 0.15–0.35 Å longer than those  $\beta$  to the methoxy group. The  $\beta$  carbons are more nucleophilic than the  $\alpha$  carbons. Consequently there is more bond formation at the  $\beta$  carbons in the transition structures.

The calculated energies, relative energies, and dipole moments of the transition structures for the cycloadditions of methyl vinyl ether are listed in Table 2. For the reactions with nitrosoethylene, nitrone, and acrolein, the endo transition structures are favored by 0.9 kcal/mol or less in the gas phase and by 1.1 kcal/mol or less in solution using the DFT method. Boger explained this endo preference in terms of hyperconjugative anomeric-type interactions in which the lone pair of electrons ( $n_O$ ) on the diene or dipole oxygen interact with the  $\sigma^*_{CO}$  orbital of the ether, therefore stabilizing the endo transition structure when arranged antiperiplanar.<sup>16</sup> In accord

(16) Boger, D. L.; Corbett, W. L.; Curran, T. T.; Kasper, A. M. *J. Am. Chem. Soc.* **1991**, *113*, 1713.

**Table 2. Calculated Energies (au), Relative Energies (kcal/mol, in Parentheses), and Dipole Moments (Debye) for Transition Structures of Cycloadditions of Methyl Vinyl Ether in Gas Phase and Solution (RHF/3-21G, Becke3LYP/6-31G\*)**

structures	RHF/3-21G			Becke3LYP/6-31G*		
	gas phase	SCRF <sup>a</sup>	dipole moment	gas phase	SCRF	dipole moment
nitrosoethylene + methyl vinyl ether						
s-cis endo	-396.316 79 (5.8)	-396.331 71 (3.5)	5.47	-400.971 44 (5.2)	-400.982 05 (3.4)	5.15
s-trans endo	-396.326 10 (0.0)	-396.337 36 (0.0)	2.80	-400.979 80 (0.0)	-400.987 54 (0.0)	3.17
s-cis exo	-396.316 29 (6.2)	-396.331 31 (3.8)	5.45	-400.972 53 (4.6)	-400.982 80 (3.0)	5.24
s-trans exo	-396.324 57 (1.0)	-396.334 89 (1.5)	2.62	-400.978 44 (0.9)	-400.985 77 (1.1)	3.00
nitron + methyl vinyl ether						
s-cis endo	-358.683 09 (6.9)	-358.693 84 (5.4)	4.86	-362.882 20 (5.7)	-362.887 99 (4.8)	3.81
s-trans endo	-358.694 12 (0.0)	-358.702 48 (0.0)	1.90	-362.891 28 (0.0)	-362.895 60 (0.0)	1.52
s-cis exo	-358.685 71 (5.3)	-358.695 89 (4.1)	4.56	-362.884 64 (4.1)	-362.890 12 (3.4)	3.23
s-trans exo	-358.691 25 (1.8)	-358.699 65 (1.8)	2.38	-362.890 03 (0.8)	-362.894 39 (0.8)	1.72
acrolein + methyl vinyl ether						
s-cis endo	-380.491 91 (5.3)	-380.502 79 (3.8)	4.29	-384.990 22 (5.8)	-384.998 33 (5.3)	4.36
s-trans endo	-380.499 63 (0.5)	-380.508 88 (0.0)	2.01	-384.999 42 (0.0)	-385.005 59 (0.0)	2.76
s-cis exo	-380.491 53 (5.5)	-380.501 48 (4.6)	2.84	-384.991 67 (4.9)	-384.999 32 (3.9)	3.86
s-trans exo	-380.500 37 (0.0)	-380.507 57 (0.8)	1.82	-384.999 20 (0.1)	-385.004 29 (0.8)	2.33
butadiene + methyl vinyl ether						
s-cis endo	-344.845 11 (2.2)	-344.850 94 (1.8)	1.58	-349.058 70 (3.3)	-349.061 69 (3.4)	1.34
s-trans endo	-344.847 09 (1.0)	-344.853 31 (0.3)	1.80	-349.063 65 (0.2)	-349.066 86 (0.1)	1.68
s-cis exo	-344.846 76 (1.2)	-344.852 43 (0.9)	1.87	-349.060 20 (2.4)	-349.063 17 (2.5)	1.75
s-trans exo	-344.848 61 (0.0)	-344.853 80 (0.0)	1.94	-349.064 01 (0.0)	-349.067 08 (0.0)	1.82

<sup>a</sup> The SCRf model uses  $\epsilon = 9.18$  D for Diels–Alder reactions and  $\epsilon = 2.14$  D for 1,3-dipolar cycloadditions. It is the same for Tables 3–5.

with this, we find that for the cycloadditions of vinyl ethers with butadiene, where there can be no such orbital interaction, the exo transition structures are favored because of the steric hindrance in the endo transition structure.

A large preference, 2.4–4.9 kcal/mol (Becke3LYP/6-31G\*), was found for the s-trans conformation of methyl vinyl ether in both the endo and exo transition structures. This preference is due to electrostatic and steric effects discussed in detail later in this paper. For the Diels–Alder reactions of methyl vinyl ether with 1-aza-1,3-butadiene, the s-trans conformation of methyl vinyl ether in the transition state is the only one reported from AM1 calculation by Fowler.<sup>2f</sup>

The Diels–Alder reactions, which have relatively non-polar transition structures, normally exhibit small solvent effects. However, for hetero-Diels–Alder cycloadditions, the transition structures have significant polarity. Solvent can effect the selectivity of Diels–Alder reaction if the different transition structures have different polarity. Table 2 lists the gas-phase dipole moments of the s-trans and s-cis transition structures. The significant difference between the dipole moments indicates that polar solvents are likely to change the relative energies of the s-trans and s-cis transition structures.

Three theoretical models including both semiempirical and ab initio methods have been reported for the modeling of solvent effects on Diels–Alder reactions.<sup>17</sup> The first model involves Monte Carlo simulations, which represent the solvent as a set of discrete molecules interacting through simple pairwise additive potentials. The supermolecule model includes a few discrete solvent molecules coordinated to the solute. Continuum cavity models such as the self-consistent reaction field (SCRf) model represents the solvent as an infinite polarizable continuum, characterized by its dielectric constant,  $\epsilon$ , surrounding a variable-shaped cavity, in which the solute is placed.

The SCRf model was used in this work to calculate the relative energy of each transition structure by single-point calculations of the transition states placed in a solvent cavity of dielectric constant 9.18 D, which is that of the common solvent methylene chloride of Diels–Alder reactions of enol ethers, or 2.14 D of benzene which is often used for 1,3-dipolar cycloadditions. The preference for the s-trans over the s-cis transition structures decreases in polar solvents. For example, for the reaction of nitrosoethylene and methyl vinyl ether, the s-trans endo transition state is 5.8 kcal/mol lower in energy than s-cis in gas phase. The difference obtained by RHF and DFT, drops to 3.5 or 3.4 kcal/mol in an SCRf cavity with  $\epsilon = 9.18$  D. The same trends are found for the other cycloadditions. The smallest effect is with the butadiene cycloadditions, where the dipole moments are rather similar for different transition states.

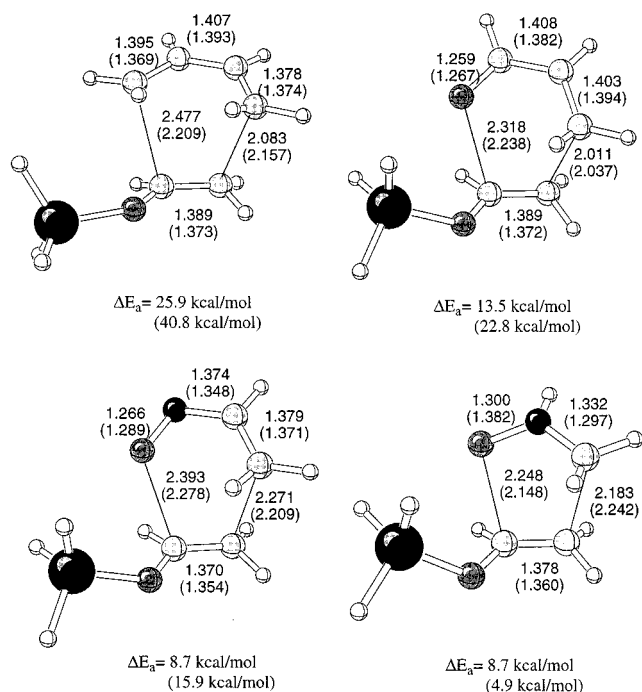
**Transition Structures for the Cycloadditions of Silyl Vinyl Ether.** For cycloadditions with silyl vinyl ether, the transition structures with the s-cis conformation could not be located. Calculations starting from an s-cis conformer did not converge or terminated at the s-trans conformation. When single-point calculations were carried out by rotating the OSiH<sub>3</sub> substituent by 180°, the energies of the s-cis conformers were found to be approximately 8 kcal/mol higher than the s-trans conformers. Figure 3 shows all of the s-trans exo transition structures for the cycloadditions of silyl vinyl ether.

The silyl vinyl ether reactions exhibit a slight preference for exo-Diels–Alder cycloadditions, in contrast to the reactions of methyl vinyl ether. This exo selectivity is consistent with Reissig's experimental results.<sup>2b</sup> The steric hindrance of the siloxy group in the endo transition structures has a greater effect than the n<sub>O</sub>– $\sigma^*_{CO}$  interaction; the exo transition structures are more stable in sterically hindered cases. Solvent effects (Table 3) do not significantly influence the exo selectivities, since there are no large differences between dipole moments of exo and endo transition structures. The SiH<sub>3</sub> group is

(17) For review of modeling methods of solvent effects on the Diels–Alder reactions, see: Cativiela, C.; Garcia, J. I.; Mayoral, J. A.; Salvatella, L. *Chem. Soc. Rev.* **1996**, 209.

**Table 3. Calculated Energies (au), Relative Energies (kcal/mol, in Parentheses), and Dipole Moments (Debye) for Transition Structures of Cycloadditions of Silyl Vinyl Ether in Gas Phase and Solution (RHF/3-21G, Becke3LYP/6-31G\*)**

structures	RHF/3-21G			Becke3LYP/6-31G*		
	gas phase	SCRf	dipole moment	gas phase	SCRf	dipole moment
nitrosoethylene + silyl vinyl ether						
s-trans endo	-646.106 65 (1.8)	-646.116 55 (1.5)	2.88	-652.398 69 (0.9)	-652.405 92 (0.2)	2.97
s-trans exo	-646.109 47 (0.0)	-646.119 01 (0.0)	2.83	652.400 05 (0.0)	-652.406 24 (0.0)	2.72
nitrone + silyl vinyl ether						
s-trans endo	-608.480 99 (0.0)	-608.489 02 (0.0)	3.44	-614.314 37 (0.0)	-614.318 33 (0.0)	2.38
s-trans exo	-698.479 74 (0.8)	-608.487 94 (0.7)	4.48	-614.314 01 (0.2)	-614.318 20 (0.1)	3.20
acrolein + silyl vinyl ether						
s-trans endo	-630.282 19 (3.7)	-630.290 18 (2.3)	1.53	-636.418 99 (1.5)	-636.424 20 (0.4)	1.92
s-trans exo	-630.288 01 (0.0)	-630.293 86 (0.0)	1.80	-636.421 37 (0.0)	-636.424 91 (0.0)	1.68
butadiene+silyl vinyl ether						
s-trans endo	-594.628 58 (0.2)	-594.632 86 (0.1)	1.13	-600.482 46 (1.8)	-600.484 72 (1.9)	0.90
s-trans exo	-594.628 94 (0.0)	-594.632 98 (0.0)	1.75	-600.485 26 (0.0)	-600.487 75 (0.0)	1.11

**Figure 3.** Transition structures and activation energies for the cycloadditions of silyl vinyl ether with butadiene, acrolein, nitrosoethylene, and nitrone with Becke3LYP/6-31G\* and RHF/3-21G (in parentheses).

predicted to be directed somewhat toward the diene or dipole, except in the case of butadiene. The dihedral angles between the SiH<sub>3</sub> moiety and the vinyl group,  $\angle C=C-O-Si$ , are in the range of 30–45°. This may be attributed to the electrostatic attraction between the silicon atom and the oxygen of the diene or dipole.<sup>18</sup>

**Transition Structures for the Cycloadditions of 1-Butene.** The reactions of 1-butene were also studied in order to enable comparison to a dienophile lacking an oxygen to influence the conformation. Table 4 gives the results. The cycloadditions of 1-butene show very small endo/exo preferences, since there are no significant orbital interactions to stabilize either transition structure. Although the s-trans preference is still observed, the differences between the s-trans and s-cis transition structures are much smaller than those for the vinyl ethers. The s-trans preferences are caused by steric

effects. Solvents exert very small effects on the relative energies of the transition structures, because the differences between the dipole moments of each transition structure are quite small. The ethyl substituent decreases the activation energies of the cycloadditions with nitrosoethylene and acrolein relative to the reactions with ethylene. The transition structures are less asynchronous than those for the vinyl ethers. The differences between the two forming bond lengths are approximately 0.1 Å (Figure 4).

**s-Trans Conformations Are Preferred in the Transition States.** The most dramatic conclusion drawn from our calculations is that the enol ether adopts the s-trans conformation in the transition state. This is especially striking in the case of methyl vinyl ether, which is known from experiment and theory to have an s-cis conformation. Therefore, for enol ethers there is a switch of conformation going from the ground state to the transition state. In the transition states of reactions with the electron-deficient nitrosoethylene, acrolein, and nitrone, the s-trans preferences are 4–6 kcal/mol in gas phase. For butadiene, the s-trans preference drops to 1–2 kcal/mol.

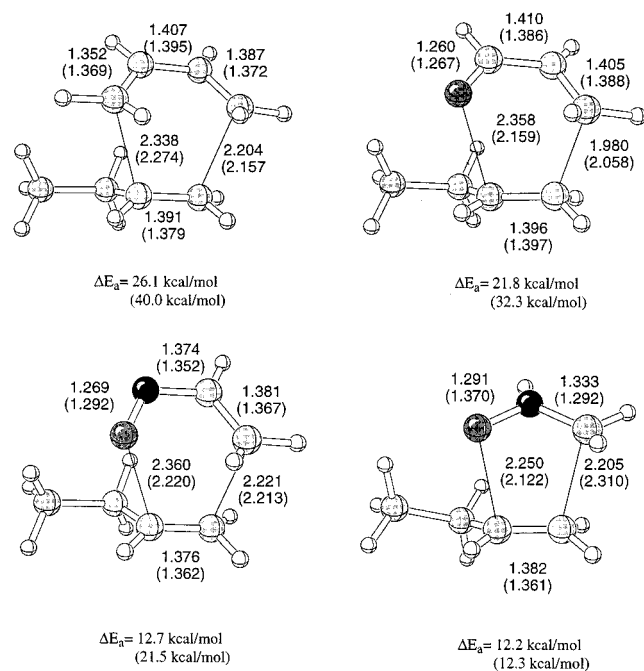
Vinyl ethers exist in the s-cis conformation to minimize the dipole interactions between the oxygen lone pairs and the  $\pi$ -system of the carbon–carbon double bond. The s-trans preference observed in the transition structures of these cycloadditions can be explained on the basis of electrostatic interactions between the lone pairs of the vinyl ether oxygens and the partial positive charge of the alkene in the transition state. This is shown qualitatively in Figure 5. The interactions with the terminal oxygens of the dienes or the nitrone might also be important. There is also a steric component to these effects which is reflected in the fact that s-cis transition structures cannot be located for silyl enol ether reactions. The 1-butene reactions have 0–3 kcal/mol preferences for the s-trans transition structures, as compared to the 0.4 kcal/mol preference for the anti conformation in the ground state.

Since the s-trans preference is due primarily to electrostatic effects, as reflected in the dipole moments of the s-cis transition structures, solvent effects are expected to be significant. Polar solvent effects reduce the s-trans preference dramatically for enol ethers, because the polar solvent stabilizes the transition structures with s-cis conformations relative to those with s-trans conformations. The solvent effects on the relatively nonpolar butene reaction are predicted to be very small.

(18) Seebach, D.; Maetzke, T.; Petter, W.; Klotzer, B.; Plattner, D. *J. Am. Chem. Soc.* **1991**, *113*, 1781.

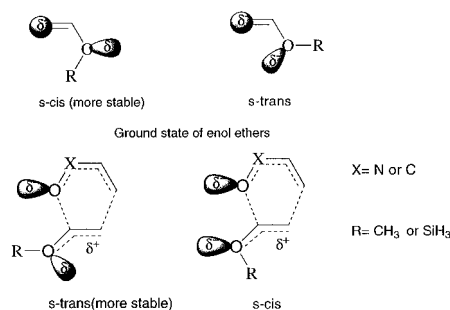
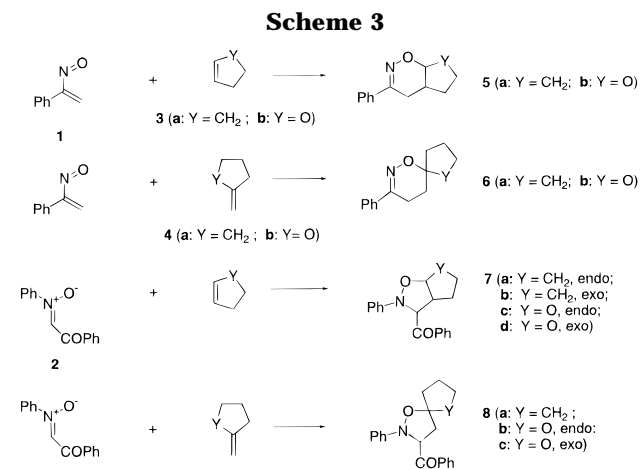
**Table 4. Calculated Energies (au), Relative Energies (kcal/mol, in Parentheses), and Dipole Moments (Debye) for Transition Structures of Cycloadditions of 1-Butene in Gas Phase and Solution (RHF/3-21G, Becke3LYP/6-31G\*)**

structures	RHF/3-21G			Becke3LYP/6-31G*		
	gas phase	SCRf	dipole moment	gas phase	SCRf	dipole moment
<b>nitrosoethylene + 1-butene</b>						
s-cis endo	-360.704 83 (2.7)	-360.712 78 (2.8)	3.51	-365.077 39 (1.8)	-365.083 23 (1.8)	3.37
s-trans endo	-360.709 25 (0.0)	-360.717 23 (0.0)	3.72	-365.080 29 (0.0)	-365.086 10 (0.0)	3.59
s-cis exo	-360.706 61 (1.0)	-360.714 25 (1.9)	3.50	-365.079 02 (0.8)	-365.085 16 (0.6)	3.52
s-trans exo	-360.708 48 (0.5)	-360.716 22 (0.6)	2.62	-365.079 77 (0.3)	-365.085 59 (0.3)	3.53
<b>nitron + 1-butene</b>						
s-cis endo	323.073 20 (2.3)	-323.080 30 (2.1)	3.25	-326.992 62 (1.8)	-326.996 34 (1.7)	2.48
s-trans endo	-323.076 82 (0.0)	-323.083 74 (0.0)	3.52	-326.995 13 (0.2)	-326.998 79 (0.2)	2.69
s-cis exo	-323.075 78 (0.7)	-323.082 57 (0.7)	3.38	-326.994 59 (0.6)	-326.998 28 (0.5)	2.48
s-trans exo	-323.076 61 (0.1)	-323.083 35 (0.2)	3.52	-326.995 48 (0.0)	-326.999 12 (0.0)	2.67
<b>acrolein + 1-butene</b>						
s-cis endo	-344.876 56 (3.6)	-344.882 23 (3.2)	2.15	-349.093 86 (2.8)	-349.097 70 (2.8)	2.33
s-trans endo	-344.881 70 (0.4)	-344.887 30 (0.0)	2.32	-349.098 23 (0.1)	-349.102 19 (0.0)	2.55
s-cis exo	-344.880 16 (1.3)	-344.884 87 (1.5)	1.94	-349.096 57 (1.1)	-349.100 16 (1.3)	2.17
s-trans exo	-344.882 30 (0.0)	-344.886 73 (0.5)	2.04	-349.098 40 (0.0)	-349.101 58 (0.4)	2.26
<b>butadiene + 1-butene</b>						
s-cis endo	-309.236 01 (1.8)	-309.238 22 (1.9)	0.70	-313.169 17 (1.5)	-313.170 55 (1.5)	0.57
s-trans endo	-309.238 94 (0.0)	-309.241 18 (0.0)	0.72	-313.171 56 (0.0)	-313.172 91 (0.0)	0.59
s-cis exo	-309.237 69 (0.8)	-309.239 93 (0.8)	0.91	-313.170 25 (0.8)	-313.171 69 (0.8)	0.77
s-trans exo	-309.237 74 (0.7)	-309.240 03 (0.7)	0.84	-313.170 73 (0.5)	-313.172 22 (0.4)	0.72

**Figure 4.** Transition structures and activation energies for the cycloadditions of 1-butene with butadiene, acrolein, nitrosoethylene, and nitron with Becke3LYP/6-31G\* and RHF/3-21G (in parentheses).

**2. Experimental Tests of the Influence of Conformation on the Rates of Cycloadditions of Enol Ethers.** There is no direct way to observe which conformation is present in the transition state of the reaction. However, these results lead to the prediction that enol ethers fixed in different conformations will react at different rates.

To test these predictions, the cycloaddition reactions of several conformationally fixed enol ethers with 1-nitroso-1-phenylethylene, **1**, and *C*-benzoyl-*N*-phenylnitron, **2**, were carried out experimentally (Scheme 3). Conformations of the enol ethers were fixed by incorporation into five-membered rings. In 2,3-dihydrofuran, **3b**, the conformation is s-cis, while in 2-methylene tetrahydrofuran, **4b**, the conformation is s-trans. Theoretically,

**Figure 5.** Electrostatic effects in the transition states of Diels-Alder with enol ethers.

the s-trans enol ether should be more reactive than the s-cis. However, the substitution patterns in 2,3-dihydrofuran (1,2-disubstituted) and 2-methylenetetrahydrofuran (1,1-disubstituted) are different, and this will influence the rates also. Therefore, controls were performed to determine the contribution of structural dissimilarity to the rate difference. Cyclopentene (**3a**) and methylenecyclopentane (**4a**) provide the appropriate models with 1,2- and 1,1-disubstitution, respectively.

Ab initio calculations were performed on these molecules to locate the Diels-Alder and 1,3-dipolar cycloaddition transition structures. RHF/3-21G calculations

**Table 5. Calculated Energies (au) and Activation Energies(kcal/mol) for Transition Structures of Cycloaddition in Gas Phase and Solution and the Dipole Moments (Debye) at RHF/3-21G**

compounds	$E$ (gas phase)	$E$ (SCRF)	dipole moment	$\Delta E_a$ (gas phase)	$\Delta E_a$ (SCRF)
cyclopentene + nitrosoethylene					
endo	-398.365 03	-398.372 93	2.72	21.0	20.5
exo	-398.366 82	-398.375 12	3.78	19.9	19.1
methylenecyclopentane + nitrosoethylene	-437.190 70	-437.198 13	3.54	18.3	18.1
dihydrofuran + nitrosoethylene					
endo	-433.978 30	-433.993 50	5.83	19.7	17.2
exo	-433.977 02	-433.992 46	5.80	20.5	17.8
2-methylenetetrahydrofuran+nitrosoethylene					
endo	-472.816 22	-472.827 02	3.25	14.0	14.8
exo	-472.814 68	-472.825 69	3.03	15.0	15.9
cyclopentene + nitrone					
endo	-360.732 33	-360.739 46	3.22	14.3	18.0
exo	-360.734 65	-360.741 67	3.34	12.8	16.7
methylenecyclopentane + nitrone	-399.557 09	-399.563 43	3.40	12.1	16.4
dihydrofuran + nitro					
endo	-396.344 71	-396.355 59	4.85	13.5	16.5
exo	-396.345 11	-396.356 50	5.11	13.2	16.0
2-methylenetetrahydrofuran + nitrone					
endo	-435.183 99	-435.190 59	1.42	7.6	13.0
exo	-435.179 42	-435.187 40	2.54	9.8	15.0

were performed for both gas and solution phase. The activation energies for each reaction and the dipole moments of these transition structures are listed in Table 5. The Diels–Alder reaction of nitrosoethylene with 2-methylenetetrahydrofuran has an activation energy which is 5.7 kcal/mol lower in the gas phase than the reaction with 2,3-dihydrofuran. In a cavity with a dielectric constant of 9.18 D, which is the  $\epsilon$  for the reaction solvent methylene chloride, this difference drops to 2.4 kcal/mol because of the higher dipole moments and solvation energies of the *s-cis* transition states. In a reaction with methylene nitrone, the reaction of 2-methylenetetrahydrofuran has an activation energy 5.6 kcal/mol lower in the gas phase and 3.0 kcal/mol lower in a cavity (with dielectric constants of 2.14 D which is the  $\epsilon$  for reaction solvent benzene) than the 2,3-dihydrofuran. The activation energies for the Diels–Alder reaction of nitrosoethylene with methylenecyclopentane are lower by 1.6 kcal/mol in the gas phase and 1.0 kcal/mol in solution relative to those of nitrosoethylene with cyclopentene. Finally, the activation energies for the 1,3-dipolar reaction of methylene nitrone with methylenecyclopentane are lower by 0.7 kcal/mol in gas phase and 0.3 kcal/mol in solution phase than those of methylene nitrone with cyclopentene.

We have carried out the Diels–Alder reactions of 1-phenyl-1-nitrosoethylene, **1**, with 2-methylenetetrahydrofuran, **4b**, 2,3-dihydrofuran, **3b**, methylenecyclopentane, **4a**, and cyclopentene, **3a**, as well as the 1,3-dipolar cycloadditions of *C*-benzoyl-*N*-phenylnitron, **2**, with each of the four alkenes (Scheme 3). 1-Nitroso-1-phenylethylene, **1**, was generated in situ by base treatment of  $\omega$ -chloroacetylbenzene oxime.<sup>19</sup> The nitrone **2**<sup>20</sup> and olefin **4b**<sup>21</sup> were prepared according to methods described in the literature. The Diels–Alder reactions were carried out in freshly distilled methylene chloride at room temperature, while the 1,3-dipolar cycloadditions were carried out in benzene. Each Diels–Alder reaction yields only one pair of enantiomers. Endo and exo products from the 1,3-dipolar reactions could be separated by flash

chromatography. All structures for pure products were verified using <sup>1</sup>H NMR, <sup>13</sup>C NMR, IR, MS, or elemental analysis. The structures of the endo products, **7c** and **8b**, were determined by X-ray crystallography.<sup>22</sup> The structures of **7a** and **7b** were determined from the coupling constants in the <sup>1</sup>H NMR. The exo/endo product ratios for the 1,3-dipolar cycloadditions were determined from isolation of the individual adducts. The endo/exo ratio was 3.2:1 for 2-methylenetetrahydrofuran, 1.1:1 for 2,3-dihydrofuran, and 1.2:1 for cyclopentene.

An endo preference is observed for the 1,3-dipolar cycloaddition of the nitrone to 2-methylenetetrahydrofuran; the 3.2:1 endo/exo ratio indicates that the endo transition structure is favored by 0.7 kcal/mol. The endo and exo products of the 1,3-dipolar cycloaddition of nitrone with 2,3-dihydrofuran and cyclopentene are formed in comparable ratios, in agreement with calculations. The energy differences predicted by RHF/3-21G between the endo and exo products in the cycloadditions of the nitrone with 2,3-dihydrofuran and cyclopentene are 1.3 and 0.5 kcal/mol, whereas the selectivity observed corresponds to a smaller endo preference.

To determine the relative rates of reactions of the enol ethers constrained to be *s-cis* and *s-trans*, the reactions of mixtures of 2,3-dihydrofuran and 2-methylenetetrahydrofuran with 1-nitroso-1-phenylethylene and with *C*-benzoyl-*N*-phenylnitron were investigated. 1-Nitroso-1-phenylethylene was reacted with a 2.5-fold excess of a mixture of the enol ethers. *C*-Benzoyl-*N*-phenylnitron was reacted with a 20-fold excess of enol ethers for the 1,3-dipolar cycloaddition competitive reactions. HPLC was used to determine the product ratios. The ratios of the relative reaction rates for 2-methylenetetrahydrofuran/2,3-dihydrofuran were 33.5 for the Diels–Alder reaction and 12.2 for the 1,3-dipolar cycloaddition. For reference, the reactions with mixtures of cyclopentene and methylenecyclopentane were also investigated. A 2.5-fold excess of a mixture of alkenes was employed for reactions with 1-nitroso-1-phenylethylene and 20-fold excess of a mixture of alkenes for reaction with *C*-benzoyl-*N*-phenylnitron. The ratios of reaction rates for meth-

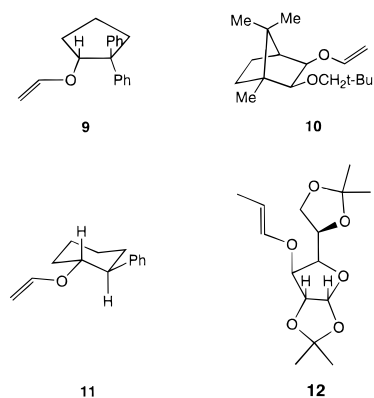
(19) For the preparation of oxime refer to: Korten, H.; Scholl, R. *Ber.* **1901**, *34*, 1901.

(20) Averas, M. C.; Cum, G.; Stragno d'Alcontres, G.; Uccella, N. *J. Chem. Soc., Perkin Trans. 1* **1972**, 222.

(21) Ireland, R. E.; Haebich, D. *Chem. Ber.* **1981**, *114*, 1418.

(22) Niwayama, S.; You, Y.; Houk, K. N.; Khan, S. *Acta Crystallogr. C* **1996**, *52*, 486.

## Scheme 4



ylenecyclopentane/cyclopentene were 13.5 for the Diels–Alder reaction and 10.4 for the 1,3-dipolar cycloaddition.

The differences in the activation energies for the 2-methylenetetrahydrofuran (s-trans conformation) and 2,3-dihydrofuran (s-cis conformation) reactions are 2.4 kcal/mol for the Diels–Alder reaction and 3.0 kcal/mol for the 1,3-dipolar cycloaddition according to RHF/3-21G calculations in the dielectric cavity. The experimental results show that the s-trans enol ether, 2-methylenetetrahydrofuran, has a lower activation energies than s-cis, dihydrofuran, by 2.1 and 1.5 kcal/mol for the Diels–Alder and 1,3-dipolar cycloadditions, respectively. The values are comparable to the calculations but show lower selectivity than predicted.

The calculated differences in activation energies for the reactions of methylenecyclopentane and cyclopentene are 1.0 kcal/mol for the Diels–Alder reaction and 0.3 kcal/mol for the 1,3-dipolar cycloaddition in solution; the differences in activation energies experimentally are 1.5 and 1.4 kcal/mol, respectively. Here the calculated values predict comparable but lower selectivity for alkene than found experimentally.

The experimental results verify the theoretical prediction of a preference for the transition states of enol ethers to be an s-trans arrangement, although when compared in solution, the preference with enol ethers is only slightly larger than the preference for alkenes. The investigation into the polarities of different solvents on the preference of the enol ether cycloaddition should be able to confirm that polar solvent can stabilize the s-cis transition state more relative to the s-trans transition state. For the Diels–Alder reaction of nitrosoethylene, there is a 1 kcal/mol greater increase in preference for reaction of the s-trans-constrained enol ether than for the alkyl model, while in the nitron cycloaddition, the experiment preference for the s-trans transition state with the ether and alkyl cases are essentially the same. The results indicate that any s-cis preference that may be present in acyclic enol ethers is eliminated in cycloaddition transition states.

**3. Implications for Stereoselectivity.** Chiral enol ethers, such as **9**, **10**, **11**, and **12** (Scheme 4), have been used in Diels–Alder cycloadditions to control  $\pi$ -facial selectivities.<sup>1</sup> Denmark et al. reported molecular mechanics calculations on the conformations of the chiral enol ethers, **9** and **10**, that they have used in Diels–Alder reactions.<sup>1c,23</sup> The s-cis conformer was predicted to be the preferred ground-state conformation. However, for the

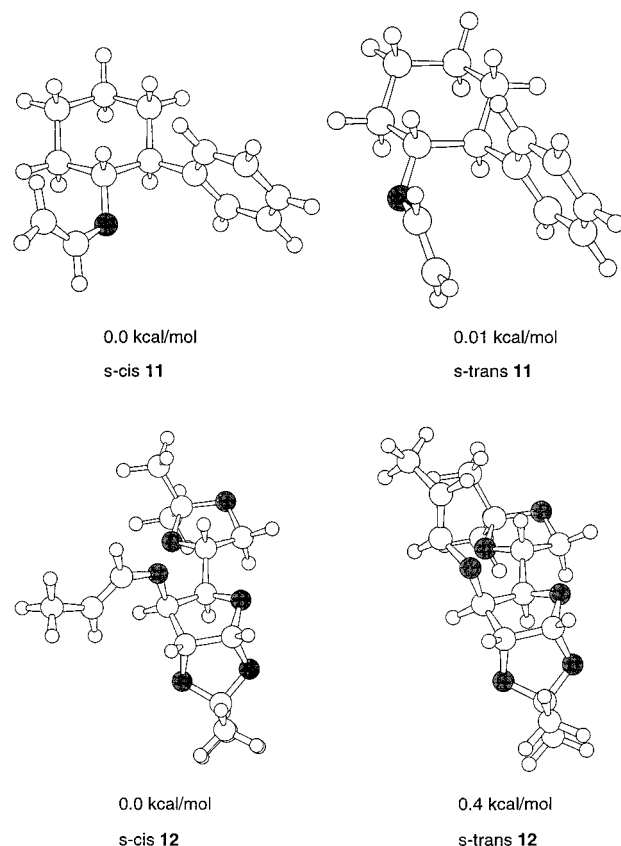


**Figure 6.** Relative energies and s-cis and s-trans conformations for the chiral enol ethers **11** and **12** optimized by the MM2\* force field.

s-cis conformer, the diene can access the enol ether from both  $\pi$ -faces in **9**, which should lead to no  $\pi$ -facial selectivity. When s-cis, the diene can access the re face of **10**, which would lead to different selectivity from that observed experimentally. Thus the stereochemical result of experiment requires the s-trans conformer to be present in the transition state.<sup>1c</sup> Denmark et al. rationalize this conformation as resulting from steric effects in the transition state.

Conformation searches were done on chiral enol ethers **11** and **12** using the MM2\* force field in MacroModel 5.0<sup>24</sup> in order to investigate whether the s-cis or s-trans conformations of these enol ethers are involved in the transition states of Diels–Alder cycloadditions. The s-cis and s-trans conformations are the ground-state conformations for both these enol ethers as shown in Figure 6. The s-cis conformation is slightly more stable than the s-trans conformation in **12**, and both are the same energy for **11**. If the transition states adopt the s-cis conformation of the enol ether, the diene would be able to access the enol ether from both the re and si faces, and there would be no selectivity. However, if the reactions take the s-trans conformation in the transition state, the re face is blocked by the other parts of the enol ether. Consequently, the transition state with the s-trans conformation of enol ether leads to the stereoselectivity observed experimentally.<sup>1</sup> The stereoselectivities of Diels–Alder reaction of chiral enol ethers proved that the

(23) Denmark, S. E.; Senanyake, C. B. W.; Ho, C.-D. *Tetrahedron* **1990**, *46*, 4857.

(24) MacroModel V5.0: Mohamadi, F.; Richards, N. G. J.; Guida, W. C.; Liskamp, R.; Lipton, M.; Caufield, C.; Chang, G.; Hendrickson, T.; Still, W. C. *J. Comput. Chem.* **1990**, *11*, 440. MM2\* is the MacroModel implementation of MM2.

enol ethers adopt the *s*-trans conformation in the cycloaddition transition states.

### Conclusion

A general type of stereoselectivity has been found for enol ethers in inverse electron-demand Diels–Alder reactions and 1,3-dipolar cycloadditions. The *s*-trans preference of enol ethers in transition structures is an electrostatic effect which decreases in polar solvents. Measurements of rates of reactions with conformationally fixed enol ethers have verified this preference. The *s*-trans transition states can explain the  $\pi$ -facial stereoselectivities in cycloadditions of chiral enol ethers observed by Denmark, Reissig, and others.

### Experimental Section

**Materials and Methods.** Commercial grade reagents and solvents were used without further purification except as indicated below. Methylene chloride and benzene were distilled from calcium hydride. *o*-Chloroacetylbenzene oxime,<sup>19</sup> *C*-benzoyl-*N*-phenylnitron,<sup>20</sup> and tetrahydro-2-methylene-2*H*-furan<sup>21</sup> were prepared by standard methods. All the reactions were stirred magnetically in oven-dried glassware under an inert atmosphere.

**General Procedure for Diels–Alder Reactions of 1-Phenyl-1-nitrosoethylene with Dienophiles.** 1-Nitroso-1-phenylethylene was formed from *o*-chloroacetylbenzene oxime in basic solution and reacts immediately with dienophiles to form Diels–Alder products.<sup>25</sup> Solutions of *o*-chloroacetylbenzene oxime (0.002 mol) and the dienophiles (cyclopentene, methylenecyclopentane, 2,3-dihydrofuran, or 2-methylenetetrahydrofuran) (0.01 mol) in methylene chloride (40 mL) were stirred with freshly ground sodium carbonate (2.12 g, 0.02 mol) at room temperature for 48 h. The reaction were stopped by removing the sodium carbonate with a Celite funnel. The solvent methylene chloride was evaporated, and the resulting oil was purified using flash chromatography.

**General Procedure for the Competitive Diels–Alder Reactions.** A solution of *o*-chloroacetylbenzene oxime (0.085 g, 0.5 mmol) and 2,3-dihydrofuran (1.25 mmol), 2-methylenetetrahydrofuran (1.25 mmol) or cyclopentene (1.25 mmol), and methylenecyclopentane (1.25 mmol) in 10 mL of methylene chloride was stirred with freshly ground sodium carbonate (5 mmol) at room temperature for 48 h. The reactions were stopped by filtering the base out of the solution and chilling the reaction mixture at 0 °C. The ratios of products formed for the competitive reactions were checked using HPLC with Nova/Pak C<sub>18</sub> column and H<sub>2</sub>O/CH<sub>3</sub>CN as solvent; pure product solutions were used as standard.

**General Procedure for the 1,3-Dipolar Cycloadditions of *C*-Benzoyl-*N*-phenylnitron.** A solution of *C*-benzoyl-*N*-phenylnitron (180 mg, 0.80 mmol) and dipolarophiles (2-methylenetetrahydrofuran, 2,3-dihydrofuran, methylenecyclopentane, or cyclopentene) (20.4 mmol) in dry benzene (3 mL) was stirred for 48 h at room temperature. The solvent was removed on rotary evaporator, and the residue was chromatographed to yield cycloadduct.

**General Procedure for the Competitive 1,3-Dipolar Cycloaddition of *C*-Benzoyl-*N*-phenylnitron.** The solution of *C*-benzoyl-*N*-phenylnitron (90 mg, 0.40 mmol) and 2-methylenetetrahydrofuran (8.0 mmol), 2,3-dihydrofuran (8.0 mmol) or methylene cyclopentane (8.0 mmol), and cyclopentene (8.0 mmol) in dry benzene (4 mL) was stirred for 48 h at room temperature. The ratios of cycloadducts formed for the competitive reactions were checked using HPLC with Nova/Pak C<sub>18</sub> column and H<sub>2</sub>O/CH<sub>3</sub>CN as solvent; pure product solutions were used as standard.

**3-Phenyl-2-aza-1-oxabicyclo[4.3.0]non-2-ene (5a):** yield = 14.3%, colorless oil. IR (KBr): 3063.8, 2939.9, 1597.3, 1446.8, 1014.7, 908.6, 760.1, 694.5 cm<sup>-1</sup>. <sup>1</sup>H NMR (CDCl<sub>3</sub>, 200 MHz): 7.63 (m, 2H), 7.33 (m, 3H), 4.00 (ddd, *J* = 8.5, 3.7, 1.9

Hz, 1H), 2.78 (dd, *J* = 17.9, 8.7 Hz, 1H), 2.29 (dd, *J* = 17.9, 4.4 Hz, 2H), 2.23 (m, 1H), 1.88 (m, 3H), 1.56 (m, 2H) ppm. <sup>13</sup>C NMR (CDCl<sub>3</sub>, 200 MHz) 160.6 (s, 1C), 135.8 (s, 1C), 129.8 (d, 1C), 128.6 (d, 2C), 125.7 (d, 2C), 78.8 (d, 1C), 37.2 (t, 1C), 32.0 (d, 1C), 31.3 (t, 1C), 24.7 (t, 1C), 22.8 (t, 1C) ppm. MW for C<sub>13</sub>H<sub>15</sub>NO: calcd 201.1154, found 201.1152.

**3-Phenyl-2-aza-1,7-dioxabicyclo[4.3.0]non-2-ene (5b):** yield = 90.0%, mp 64–65 °C. IR (KBr): 3063.8, 2982.5, 2941.8, 2905.2, 1592.8, 1446.8, 1080.3, 979.9, 897.1, 762.0, 700.2 cm<sup>-1</sup>. <sup>1</sup>H NMR (DCCl<sub>3</sub>, 200 MHz) 7.73 (m, 2H), 7.41 (m, 3H), 5.66 (d, *J* = 6.1 Hz, 1H), 4.04 (ddd, *J* = 15.3, 7.2, 2.1 Hz, 1H), 3.89 (ddd, *J* = 15.3, 7.4, 1.8 Hz, 1H), 2.93 (m, 1H), 2.74 (d, *J* = 4.9 Hz, 2H), 2.18 (m, 1H), 1.77 (m, 1H) ppm. <sup>13</sup>C NMR (CDCl<sub>3</sub>, 200 MHz) 164.9 (s, 1C), 135.0 (s, 1C), 130.4 (d, 1C), 128.8 (d, 2C), 125.9 (d, 2C), 102.1 (t, 1C), 68.4 (d, 1C), 37.0 (t, 1C), 30.3 (d, 1C), 25.1 (t, 1C) ppm. MW for C<sub>12</sub>H<sub>13</sub>NO<sub>2</sub>: calcd 203.0946, found 203.0950.

**3-Phenyl-2-aza-1-oxaspiro[5.4]dec-2-ene (6a):** yield = 83.8%, mp 62–63 °C. IR (KBr): 3063.8, 2961.1, 2870.1, 1592.5, 1446.8, 1012.8, 910.5, 754.3, 688.7 cm<sup>-1</sup>. <sup>1</sup>H NMR (CDCl<sub>3</sub>, 200 MHz) 7.62 (m, 2H), 7.29 (m, 3H), 2.57 (t, *J* = 6.9 Hz, 2H), 1.89 (t, *J* = 6.9 Hz, 2H), 1.81 (m, 4H), 1.61 (m, 2H), 1.19 (m, 2H) ppm. <sup>13</sup>C NMR (CDCl<sub>3</sub>): 153.7 (s, 1C), 136.2 (s, 1C), 129.3 (d, 1C), 128.4 (d, 2C), 125.2 (d, 2C), 85.2 (s, 1C), 37.0 (t, 2C), 28.1 (t, 1C), 24.4 (t, 2C), 20.9 (t, 1C) ppm. MW for C<sub>14</sub>H<sub>17</sub>NO<sub>2</sub>: calcd 215.1310, found 215.1311.

**3-Phenyl-2-aza-1,7-dioxaspiro[5.4]dec-2-ene (6b):** yield = 95.6%, mp 47–48 °C. IR (KBr): 3063.8, 2988.7, 2951.1, 2926.1, 2876.2, 1593.8, 1444.9, 1080.3, 983.8, 773.6, 702.2 cm<sup>-1</sup>. <sup>1</sup>H NMR (CDCl<sub>3</sub>, 200 MHz) 7.72 (m, 2H), 7.35 (m, 3H), 4.03 (m, 2H), 2.76 (m, 2H), 2.25 (m, 2H), 2.08 (m, 2H), 1.90 (m, 2H) ppm. <sup>13</sup>C NMR (CDCl<sub>3</sub>, 200 MHz) 154.8 (s, 1C), 135.6 (s, 1C), 129.5 (d, 1C), 128.4 (d, 2C), 125.5 (d, 2C), 104.8 (s, 1C), 68.1 (t, 1C), 35.8 (t, 1C), 26.3 (t, 1C), 24.2 (t, 1C), 20.4 (t, 1C) ppm. MW for C<sub>13</sub>H<sub>15</sub>NO<sub>2</sub>: calcd 217.1103, found 217.1100.

**(3 $\alpha$ ,3 $\alpha$ ,6 $\alpha$ )-3-Benzoyl-2-phenylcyclopent[2,1-*d*]tetrahydroisoxazole (7a):** yield = 46.2%, mp 153–154 °C. IR (thin film): 3063, 2957, 2870, 1694, 1672, 1597, 1580, 1491, 1275, 1180, 1026, 756, 692 cm<sup>-1</sup>. <sup>1</sup>H NMR (400 Hz, CDCl<sub>3</sub>): 1.60–1.67 (m, 2H), 1.74–1.91 (m, 3H), 2.02–2.08 (m, 2H), 3.24–3.29 (m, 1H), 4.20 (d, *J* = 6.1 Hz, 1H), 4.95 (dd, *J* = 6.0, 5.2 Hz, 1H), 6.94 (t, *J* = 7.4 Hz, 1H), 6.99 (dd, *J* = 8.7, 1.1 Hz, 2H), 7.21 (dd, *J* = 8.7, 7.4 Hz, 2H), 7.48 (dd, *J* = 8.4, 7.4 Hz, 2H), 7.59 (t, 7.4 Hz, 1H), 8.19 (dd, *J* = 8.4, 1.2 Hz, 2H) ppm. <sup>13</sup>C NMR (400 Hz, CDCl<sub>3</sub>): 24.1 (t, 1C), 31.5 (t, 1C), 32.1 (t, 1C), 50.3 (d, 1C), 78.1 (d, 1C), 84.0 (d, 1C), 116.4 (d, 2C), 122.6 (d, 1C), 128.8 (d, 2C), 128.8 (d, 2C), 129.2 (d, 2C), 133.7 (d, 1C), 135.2 (s, 1C), 149.2 (s, 1C), 197.3 (s, 1C) ppm. Anal. Calcd. for C<sub>19</sub>H<sub>19</sub>NO<sub>2</sub>: C, 77.79; H, 6.53; N, 4.77. Found: C, 77.54; H, 6.46; N, 4.72.

**(3 $\beta$ ,3 $\alpha$ ,6 $\alpha$ )-3-Benzoyl-2-phenylcyclopent[2,1-*d*]tetrahydroisoxazole (7b):** yield = 37.8%, mp 138–139 °C. IR (thin film): 3063, 2957, 2872, 1688, 1597, 1579, 1491, 1449, 1275, 1236, 1211, 1182, 1159, 1026, 988, 752, 691 cm<sup>-1</sup>. <sup>1</sup>H NMR (400 Hz, CDCl<sub>3</sub>): 1.38–1.43 (m, 1H), 1.50–1.60 (m, 2H), 1.71–1.89 (m, 2H), 2.01–2.07 (m, 1H), 3.46 (dddd, *J* = 9.0, 5.9, 5.8, 3.0 Hz, 1H), 4.79 (ddd, *J* = 7.0, 5.8, 1.6 Hz, 1H), 5.23 (d, *J* = 9.0 Hz, 1H), 6.93 (t, *J* = 7.3 Hz, 1H), 6.97 (dd, *J* = 8.8, 1.1 Hz, 2H), 7.23 (dd, *J* = 8.8, 7.3 Hz, 2H), 7.51 (dd, *J* = 8.4, 7.5 Hz, 2H), 7.61 (t, 7.5 Hz, 1H), 8.02 (dd, *J* = 8.4, 1.2 Hz, 2H) ppm. <sup>13</sup>C NMR (400 Hz, CDCl<sub>3</sub>): 25.5 (t, 1C), 27.9 (t, 1C), 30.6 (t, 1C), 52.5 (d, 1C), 75.0 (d, 1C), 84.8 (d, 1C), 114.6 (d, 2C), 121.8 (d, 1C), 128.5 (d, 2C), 128.9 (d, 2C), 128.9 (d, 2C), 133.6 (d, 1C), 136.1 (s, 1C), 151.3 (s, 1C), 196.0 (s, 1C) ppm. Anal. Calcd. for C<sub>19</sub>H<sub>19</sub>NO<sub>2</sub>: C, 77.79; H, 6.53; N, 4.77. Found: C, 77.68; H, 6.67; N, 4.58.

**(3 $\alpha$ ,3 $\alpha$ ,6 $\alpha$ )-3-Benzoylhexahydro-2-phenylfuro[3,2-*d*]isoxazole (7c):** yield = 51%, mp 133–134 °C. IR (thin film): 3062, 2969, 2894, 1692, 1597, 1489, 1219, 1078, 1016, 922, 789, 754 cm<sup>-1</sup>. <sup>1</sup>H NMR (400 Hz, CDCl<sub>3</sub>): 1.97–2.02 (m, 1H), 2.14–2.17 (m, 1H), 3.50–3.52 (m, 1H), 3.72 (dt, *J* = 9.2, 7.3 Hz, 1H),

(25) (a) Faragher, R.; Gilchrist, T. L. *J. Chem. Soc., Perkin Trans. 1* 1979, 249. (b) Gilchrist, T. L. *Chem. Soc. Rev.* 1983, 79, 53.

3.85 (ddd,  $J = 9.2, 8.6, 2.2$  Hz, 1H), 5.07 (d,  $J = 2.2$  Hz, 1H), 6.01 (d,  $J = 5.3$  Hz, 1H), 6.93 (t,  $J = 7.3$  Hz, 1H), 7.11 (dd,  $J = 8.7, 1.0$  Hz, 2H), 7.25 (dd,  $J = 8.7, 7.3$  Hz, 2H), 7.46 (dd,  $J = 8.4, 7.4$  Hz, 2H), 7.57 (t, 7.4 Hz, 1H), 8.02 (dd,  $J = 8.4, 1.2$  Hz, 2H) ppm.  $^{13}\text{C}$  NMR (400 Hz,  $\text{CDCl}_3$ ): 31.1 (t, 1C), 50.3 (d, 1C), 68.3 (t, 1C), 73.8 (d, 1C), 108.9 (d, 1C), 114.4 (d, 2C), 121.7 (d, 1C), 128.8 (d, 2C), 128.8 (d, 2C), 128.9 (d, 2C), 133.6 (d, 1C), 135.0 (s, 1C), 149.6 (s, 1C), 196.0 (s, 1C) ppm. Anal. Calcd for  $\text{C}_{18}\text{H}_{17}\text{NO}_3$ : C, 73.20; H, 5.80; N, 4.75. Found: C, 72.87; H, 5.65; N, 4.57.

**(3 $\beta$ ,3 $\alpha$ ,6 $\alpha$ )-3-Benzoylhexahydro-2-phenylfuro[3,2-*d*]-isoxazole (7d):** yield = 47%, mp 176–178 °C. IR (thin film): 3064, 2976, 2892, 1690, 1597, 1491, 1252, 1076, 1024, 926, 799, 750  $\text{cm}^{-1}$ .  $^1\text{H}$  NMR (400 Hz,  $\text{CDCl}_3$ ): 1.74–1.85 (m, 2H), 3.68–3.70 (m, 1H), 3.98 (ddd,  $J = 10.9, 7.7, 2.0$  Hz, 1H), 4.25 (ddd,  $J = 10.9, 7.9, 2.4$  Hz, 1H), 4.96 (d,  $J = 8.1$  Hz, 1H), 5.96 (d,  $J = 5.3$  Hz, 1H), 7.04 (t,  $J = 7.3$  Hz, 1H), 7.09 (dd,  $J = 8.7, 1.1$  Hz, 2H), 7.24 (dd,  $J = 8.7, 7.3$  Hz, 2H), 7.46 (dd,  $J = 8.6, 7.4$  Hz, 2H), 7.57 (t, 7.4 Hz, 1H), 8.02 (dd,  $J = 8.6, 1.4$  Hz, 2H) ppm.  $^{13}\text{C}$  NMR (400 Hz,  $\text{CDCl}_3$ ): 28.8 (t, 1C), 51.1 (d, 1C), 69.6 (t, 1C), 72.9 (d, 1C), 105.1 (d, 1C), 118.7 (d, 2C), 124.3 (d, 1C), 128.4 (d, 2C), 128.7 (d, 2C), 129.2 (d, 2C), 134.2 (d, 1C), 135.6 (s, 1C), 148.5 (s, 1C), 194.2 (s, 1C) ppm. Anal. Calcd for  $\text{C}_{18}\text{H}_{17}\text{NO}_3$ : C, 73.20; H, 5.80; N, 4.75. Found: C, 72.90; H, 5.82; N, 4.61.

**3-Benzoyl-*N*-phenyl-2-aza-1-oxaspiro[4.4]nonane (8a):** yield = 85%, mp 84–85 °C. IR (thin film): 3063, 2961, 2872, 1696, 1674, 1597, 1449, 1337, 1219, 1182, 910, 752, 731, 692  $\text{cm}^{-1}$ .  $^1\text{H}$  NMR (400 Hz,  $\text{CDCl}_3$ ): 1.41–1.50 (m, 1H), 1.60–1.71 (m, 2H), 1.80–1.93 (m, 4H), 2.12–2.18 (m, 1H), 2.69 (dd,  $J = 12.0, 8.5$  Hz, 1H), 2.72 (dd,  $J = 12.0, 8.3$  Hz, 1H), 4.90 (dd,  $J = 8.5, 8.3$  Hz, 1H), 6.87 (t,  $J = 7.3$  Hz, 1H), 6.94 (dd,  $J = 8.8, 1.0$  Hz, 2H), 7.22 (dd,  $J = 8.8, 7.3$  Hz, 2H), 7.47 (dd,  $J = 8.4, 7.4$  Hz, 2H), 7.58 (t, 7.4 Hz, 1H), 8.20 (dd,  $J = 8.4, 1.2$  Hz, 2H) ppm.  $^{13}\text{C}$  NMR (400 Hz,  $\text{CDCl}_3$ ): 24.0 (t, 1C), 24.4 (t, 1C), 35.8 (t, 1C), 37.2 (t, 1C), 44.4 (t, 1C), 71.9 (d, 1C), 92.8 (s, 1C), 113.4 (d, 2C), 120.9 (d, 1C), 128.6 (d, 2C), 128.8 (d, 2C), 129.3 (d, 2C), 134.4 (d, 1C), 134.4 (s, 1C), 151.8 (s, 1C), 198.0 (s, 1C) ppm. Anal. Calcd for  $\text{C}_{20}\text{H}_{21}\text{NO}_2$ : C, 78.15; H, 6.89; N, 4.56. Found: C, 78.41; H, 7.02; N, 4.43.

***trans*-3-Benzoyl-*N*-phenyl-2-aza-1,6-dioxaspiro[4.4]-nonane (8b):** yield = 72%, mp 99–100 °C. IR (thin film):

3061, 2984, 2957, 2890, 1696, 1674, 1582, 1489, 1449, 1213, 1180, 1159, 1094, 1082, 1026, 982, 783, 729, 694  $\text{cm}^{-1}$ .  $^1\text{H}$  NMR (400 Hz,  $\text{CDCl}_3$ ): 1.96–2.04 (m, 1H), 2.11–2.28 (m, 2H), 2.30–2.39 (m, 1H), 2.82 (d,  $J = 8.3$  Hz, 2H), 3.89–3.99 (m, 2H), 5.17 (t,  $J = 8.3$  Hz, 1H), 6.92 (t,  $J = 7.3$  Hz, 1H), 6.96 (d,  $J = 7.8$  Hz, 2H), 7.24 (dd,  $J = 7.8, 7.3$  Hz, 2H), 7.48 (dd,  $J = 7.7, 7.4$  Hz, 2H), 7.59 (t, 7.4 Hz, 1H), 8.14 (d,  $J = 7.7$  Hz, 2H) ppm.  $^{13}\text{C}$  NMR (360 Hz,  $\text{CDCl}_3$ ): 24.5 (t, 1C), 32.3 (t, 1C), 42.4 (t, 1C), 67.8 (t, 1C), 71.1 (d, 1C), 113.6 (d, 2C), 114.6 (s, 1C), 121.4 (d, 1C), 128.7 (d, 2C), 128.8 (d, 2C), 129.2 (d, 2C), 133.7 (d, 1C), 134.7 (s, 1C), 152.7 (s, 1C), 197.3 (s, 1C) ppm. Anal. Calcd for  $\text{C}_{19}\text{H}_{19}\text{NO}_3$ : C, 73.77; H, 6.18; N, 4.53. Found: C, 73.63; H, 6.09; N, 4.44.

***cis*-3-Benzoyl-*N*-phenyl-2-aza-1,6-dioxaspiro[4.4]nonane (8c):** yield = 23.0%, mp 133–134 °C. IR (thin film): 3063, 2955, 2886, 1698, 1671, 1491, 1339, 1277, 1211, 1182, 1159, 1088, 954, 758, 692  $\text{cm}^{-1}$ .  $^1\text{H}$  NMR (400 Hz,  $\text{CDCl}_3$ ): 1.89–2.00 (m, 1H), 2.03–2.20 (m, 2H), 2.23–2.34 (m, 1H), 2.85 (dd,  $J = 13.1, 6.2$  Hz, 1H), 2.91 (dd,  $J = 13.1, 10.1$  Hz, 1H), 3.96–4.01 (m, 1H), 4.10–4.15 (m, 1H), 4.78 (dd,  $J = 10.1, 6.2$  Hz, 1H), 6.96 (t,  $J = 7.3$  Hz, 1H), 7.00 (dd,  $J = 8.7, 1.0$  Hz, 2H), 7.23 (dd,  $J = 8.7, 7.3$  Hz, 2H), 7.45 (dd,  $J = 8.6, 7.4$  Hz, 2H), 7.56 (t, 7.4 Hz, 1H), 8.17 (d,  $J = 8.6$  Hz, 2H) ppm.  $^{13}\text{C}$  NMR (360 Hz,  $\text{CDCl}_3$ ): 25.1 (t, 1C), 35.0 (t, 1C), 43.3 (t, 1C), 69.1 (t, 1C), 72.5 (d, 1C), 113.0 (s, 1C), 116.6 (d, 2C), 123.4 (d, 1C), 128.6 (d, 2C), 128.8 (d, 2C), 129.3 (d, 2C), 134.2 (d, 1C), 135.6 (s, 1C), 150.8 (s, 1C), 197.2 (s, 1C) ppm. Anal. Calcd for  $\text{C}_{19}\text{H}_{19}\text{NO}_3$ : C, 73.77; H, 6.18; N, 4.53. Found: C, 73.83; H, 5.92; N, 4.26.

**Acknowledgment.** We are grateful to the National Institute of General Medical Sciences, National Institutes of Health, for financial support of this research, to Professor Hans-Ulrich Reissig for bringing this problem to our attention, and to the UCLA Office of Academic Computing and the National Center for Supercomputing Applications (NCSA) for the computer time used for this work.

JO971408Q